

AD-A046 363

BENDIX CORP TETERBORO N J FLIGHT SYSTEMS DIV  
GLIDE PATH AUGMENTATION WITH INERTIAL FLIGHT PATH ANGLE.(U)  
DEC 74 V MUEHTER

F/G 1/2

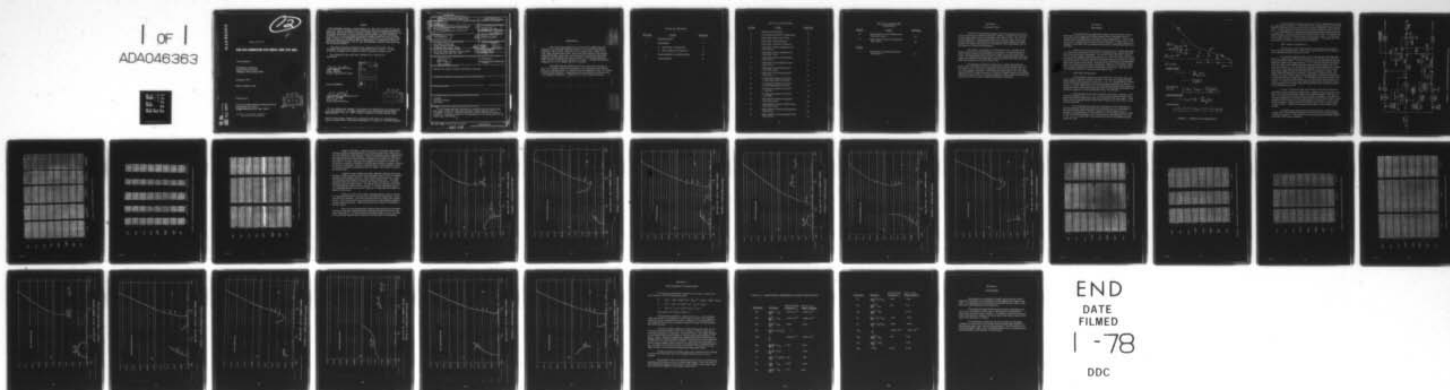
UNCLASSIFIED

AFFDL-TR-77-72

F33615-72-C-1753

NL

1 OF 1  
ADA046363



END  
DATE  
FILMED  
1 -78  
DDC

AD A046363

12

AFFDL-TR-77-72

## GLIDE PATH AUGMENTATION WITH INERTIAL FLIGHT PATH ANGLE

Vincent Muehter

The Bendix Corporation  
Flight Systems Division  
Teterboro, New Jersey 07608

December 1974

FINAL REPORT A005

Prepared for:

Air Force Flight Dynamics Laboratory/FGT  
United States Air Force  
Wright-Patterson AFB, Ohio 45433

APPROVED FOR PUBLIC RELEASE;  
DISTRIBUTION UNLIMITED

DDC  
RECEIVED  
NOV 9 1977  
D

AD NO. \_\_\_\_\_  
DDC FILE COPY: \_\_\_\_\_

# NOTICE

When Government drawings, specifications, or other data are used for any purpose other than in connection with a definitely related Government procurement operation, the United States Government thereby incurs no responsibility nor any obligation whatsoever, and the fact that the government may have formulated, furnished, or in any way supplied the said drawings, specifications, or other data, is not to be regarded by implication or otherwise as in any manner licensing the holder or any other person or corporation, or conveying any rights or permission to manufacture, use, or sell any patented invention that may in any way be related thereto.

This report has been reviewed by the Information Office (OI) and is releasable to the National Technical Information Service (NTIS). At NTIS it will be available to the general public, including foreign nations.

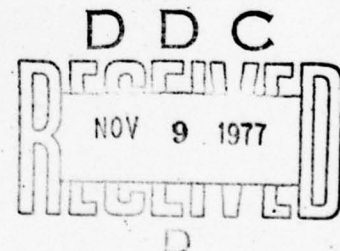
This technical report has been reviewed and is approved for publication.

*Jim J. Guckian*  
JIM J. GUCKIAN  
Project Engineer  
Terminal Area Control Branch

ACCESSION for	
NTIS	White Section <input checked="" type="checkbox"/>
DDC	Buff Section <input type="checkbox"/>
UNANNOUNCED	<input type="checkbox"/>
JUSTIFICATION	
BY	
DISTRIBUTION/AVAILABILITY CODES	
Dist.	AVAIL. and/or SPECIAL
A	

FOR THE COMMANDER

*Robert P. Johannes*  
ROBERT P. JOHANNES  
Acting Chief  
Flight Control Division



"If your address has changed, if you wish to be removed from our mailing list, or if the addressee is no longer employed by your organization please notify AFDDL/STINFO, W-P AFB, OH 45433 to help us maintain a current mailing list".

Copies of this report should not be returned unless return is required by security considerations, contractual obligations, or notice on a specific document.

UNCLASSIFIED

SECURITY CLASSIFICATION OF THIS PAGE (When Data Entered)

19 REPORT DOCUMENTATION PAGE		READ INSTRUCTIONS BEFORE COMPLETING FORM	
18 REPORT NUMBER AFFDL-TR-77-72	2. GOVT ACCESSION NO.	3. RECIPIENT'S CATALOG NUMBER	
4. TITLE (and Subtitle) GLIDE PATH AUGMENTATION WITH INERTIAL FLIGHT PATH ANGLE		9. TYPE OF REPORT & PERIOD COVERED Final <i>rept.</i> Jan 1972 - Dec 1974	
7. AUTHOR(s) Vincent Muehter		8. CONTRACT OR GRANT NUMBER(s) F33615-72-C-1753	
9. PERFORMING ORGANIZATION NAME AND ADDRESS The Bendix Corporation Flight Systems Division Teterboro, New Jersey 07608		10. PROGRAM ELEMENT, PROJECT, TASK AREA & WORK UNIT NUMBERS 62201F 82260121	
11. CONTROLLING OFFICE NAME AND ADDRESS Air Force Flight Dynamics Laboratory/FGT Wright-Patterson AFB, OH 45433		12. REPORT DATE December 1974	
14. MONITORING AGENCY NAME & ADDRESS (if different from Controlling Office) 1236p.		13. NUMBER OF PAGES 34	
		15. SECURITY CLASS. (of this report) Unclassified	
		15a. DECLASSIFICATION/DOWNGRADING SCHEDULE	
16. DISTRIBUTION STATEMENT (of this Report) Approved for public release; distribution unlimited			
17. DISTRIBUTION STATEMENT (of the abstract entered in Block 20, if different from Report)			
18. SUPPLEMENTARY NOTES			
19. KEY WORDS (Continue on reverse side if necessary and identify by block number) Automatic Aircraft Landings Wind Shear			
20. ABSTRACT (Continue on reverse side if necessary and identify by block number) A two segment approach configuration using inertially derived flight path angle to damp the glide path and upper segment approach paths is developed in the text. System performance in both head and tail winds is evaluated. Stability analysis is also presented on root locus plots for the capture and track modes.			

409 146



## FOREWORD

This report was prepared for the Air Force Flight Dynamics Laboratory by the Flight Systems Division, The Bendix Corporation, Teterboro, New Jersey, under Air Force Contract No. F33615-72-C-1753, data document item A005, Glide Path Augmentation with Inertial Flight Path Angle. This work was performed in conjunction with other program tasks during the time period January 1972 through December 1974. The Air Force Project Manager was Capt. T. Imrich with Project Engineers Lt. R. P. Denaro and Lt. B. Kunciw.

The Flight Systems Division effort was under the direction of Mr. F. G. Adams, principal investigator. The simulation and analysis task was conducted by Mr. V. Muehter with contributions by Mr. K. Moses, Assistant Chief Engineer. Supporting data and configuration requirements were supplied by Messrs. J. Woloshen, M. Sforza and S. Skaritka.

## TABLE OF CONTENTS

<u>SECTION</u>	<u>TITLE</u>	<u>PAGE NO.</u>
1	INTRODUCTION	1
2	DISCUSSION	2
	1. Glide Slope Configuration	2
	2. Upper Segment Configuration	4
3	DEVELOPMENT OF SIMULATION	26
4	CONCLUSIONS	29

# LIST OF ILLUSTRATIONS

<u>FIGURE</u>	<u>TITLE</u>	<u>PAGE NO.</u>
1	Control Law Derivation	3
2	Two Segment Approach Configuration	5
3	Glide Slope Capture and Track	6
4	Glide Slope Track Response	7
5	Glide Slope Turbulence Response	8
6	Glide Slope Capture Integrator Gain Root Locus	10
7	Glide Slope Capture Displacement Gain Root Locus	11
8	Glide Slope Capture Damping Gain Root Locus	12
9	Glide Slope Track Integrator Gain Root Locus	13
10	Glide Slope Track Displacement Gain Root Locus	14
11	Glide Slope Track Damping Gain Root Locus	15
12	Two Segment Capture and Track (Initial Intercept from Below)	16
13	Two Segment Capture and Track (Initial Intercept from Above)	17
14	Two Segment Capture and Track (Close In)	18
15	Two Segment Capture and Track (Far Out)	19
16	Upper Segment Capture Integrator Gain Root Locus	20
17	Upper Segment Capture Displacement Gain Root Locus	21
18	Upper Segment Capture Damping Gain Root Locus	22
19	Upper Segment Track Integrator Gain Root Locus	23

LIST OF ILLUSTRATIONS  
( CONTINUED)

<u>FIGURE</u>	<u>TITLE</u>	<u>PAGE NO.</u>
20	Upper Segment Track Displacement Gain Root Locus	24
21	Upper Segment Track Damping Gain Root Locus	25
 <u>TABLE</u>		
1	Longitudinal Dimensional Stability Derivatives	27



## SECTION 1

### INTRODUCTION

The KC-135 development program has been primarily concerned with improvement of automatic approach, landing, and takeoff performance through optimization of the roll and pitch axis control loops. The roll axis work included use of inertial drift angle in the localizer mode and during runway alignment. Test flight data obtained during the lateral axis flights pointed to a needed improvement in the stability of the longitudinal axis in the presence of shears and turbulence.

This study, in response to contract item A005, "Inertial Glide Slope Augmentation" was performed to investigate a conceptual design approach using inertially derived flight path angle to damp the glide slope mode. The design task was to provide a system design that would gradually reduce the authority of the glide path signal and employ the flight path angle signal for guidance to the flare engage point.

An extension of this basic study was to replace the glide path signal with a signal derived from vertical and horizontal position data such as  $h$  and  $X$  or  $R$ . This work is identified as the upper segment (U/S) portion of the approach problem. Combining the glide slope ( $2.75^\circ$ ) and upper segment ( $3^\circ$ - $6^\circ$ ) modes resulted in a typical two segment approach geometry, where the objective was to accomplish captures of these upper and lower segments from above or below without undesirable overshoots.

## SECTION 2

### DISCUSSION

The present KC-135 glide slope capture and track mode utilizes a fixed beam error engage point supplemented with an  $\dot{h}$  damping term for track and an  $\dot{h}$  command bias to improve capture performance. This configuration and its development is described in report A009 of this contract. The use of  $\dot{h}$  as a damping term during track has a tendency to oppose necessary changes in sink rate, due to horizontal wind shears, causing departures from the beam.

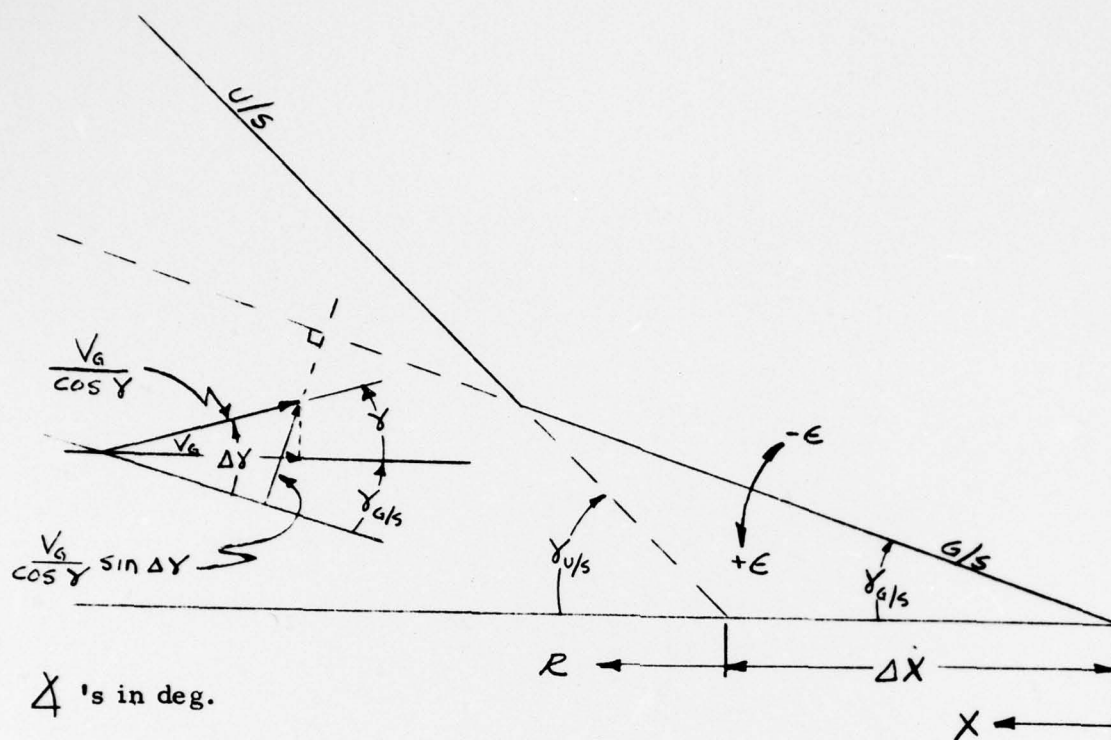
With the above characteristics in mind, the use of flight path angle ( $\gamma$ ) information to provide a rate term for damping during capture and track has some very definite advantages. The use of a beam rate term, derived from  $\gamma$ , during capture would allow the use of a control law which could avoid overshoots by automatically adjusting the engage point as a function of closure rate on the beam. Also, the use of  $\gamma (\dot{h}/V_G)$  as a damping term during glide slope track would provide beam oscillation damping, as well as the  $\dot{h}$  could, since  $V_G$  would not vary at those frequencies. However, it would also allow the aircraft to respond favorably to horizontal wind shears, since the sink rate would be allowed to vary with ground speed ( $V_G$ ).

#### 1. Glide Slope Configuration

An exponential control law was proposed to accomplish upper and lower segment captures without overshoots. For the lower segment (glide slope) captures the control law used was  $\epsilon + \tau \dot{\epsilon} = 0$ . The derivation of beam rate from inertial flight path ( $\gamma$ ) and ground speed information is shown in Figure 1. In this study beam error was desensitized linearly with range from 42,000 feet while the derived beam rate term was effectively desensitized by fixing the range term in the denominator at  $X_0 = 42,000$  feet.

Once the glide slope (G/S) mode has been armed, capture is automatically initiated when  $\epsilon + \tau \dot{\epsilon} = 0$ , since the aircraft at that instant is tangent to the desired exponential path for its particular intercept angle. Glide slope track is engaged twenty seconds after a beam error very close to zero has been attained.

As an example of how the above technique could be extended for control along any chosen upper segment, without the use of a fixed beam, a derivation is also shown in Figure 1 where an effective beam error is derived. Desensitization was accomplished by multiplying through by range to effectively obtain altitude error and rate terms, permitting the use of  $h_e + \tau \dot{h}_e = 0$ , as a control law, since beam error has no real physical meaning in this case.



#### GLIDE SLOPE

$$\epsilon + \tau \dot{\epsilon} = \epsilon - \tau \frac{\frac{V_G}{\cos \gamma} \sin \Delta \gamma}{X}$$

$$\cong \epsilon - \tau \frac{V_G (\gamma_{GS} + \gamma)}{X}$$

Desensitizing  
from  $X_0$ ;

$$\boxed{[\epsilon + \tau \dot{\epsilon}]_{des} = [\epsilon]_{des} + \tau \frac{V_G (\gamma_{GS} + \gamma)}{X_0}}$$

#### UPPER SEGMENT

$$\epsilon + \tau \dot{\epsilon} = (\gamma_{u/s} - 57.3 \frac{h}{R}) - \tau \frac{\frac{V_G}{\cos \gamma} \sin \Delta \gamma}{R}$$

Desensitizing;

$$\boxed{h_{\epsilon} + \tau \dot{h}_{\epsilon} = R(\epsilon + \tau \dot{\epsilon}) = R\gamma_{u/s} - 57.3 h - \tau V_G (\gamma_{u/s} + \gamma)}$$

FIGURE 1. CONTROL LAW DERIVATION



The resulting two segment capture and track configurations studied are represented in Figure 2. The portion of the configuration with which this report is primarily concerned is the lower portion designated "G/S Computations". In this portion it is shown that during G/S capture the control law is  $(\epsilon + \tau_2 \dot{\epsilon})$  desensitized, commanding pitch attitude through displacement and integral paths. During the G/S track mode the beam error ( $\epsilon$ ) displacement loop is tightened by an increase in gain, derived beam rate ( $\dot{\epsilon}$ ) is retained for damping, and pure  $\epsilon$  is fed through the integrator. The tightening of the beam loop is necessary for good shear performance.

## 2. Upper Segment Configuration

The operation of the upper segment computations are similar to that of the glide slope portion. In this case a gain change was not required in the displacement loop during U/S track.

The required system inputs for this configuration are flight path angle ( $\gamma$ ), range from glide slope transmitter ( $X$ ), ground speed ( $V_G$ ) and two pilot selected inputs. The first of these two would establish the desired flight path angle of the upper segment ( $\gamma$  u/s) while the second would determine the range offset between the upper segment and the glide slope ( $\Delta X$ , reference Figure 1). The Asymptote Intercept Altitude Indicator is coupled to these two pilot inputs to continuously indicate to the pilot his minimum glide slope engage altitude for the particular combination of inputs. The Upper Segment Engage Point Indicator continuously indicates to the pilot whether or not his chosen upper segment geometry is attainable based upon his present position and trajectory. An attainable trajectory would be indicated by the indicator approaching zero, at which point capture would be initiated. An interlock to the upper segment engage logic is included to preclude engagement of an upper segment capture when the aircraft is already below the glide slope beam.

Figure 3 depicts the glide slope capture and track performance attainable with the proposed configuration. Captures were performed from below at a maximum intercept angle from horizontal flight at 1500 feet, under no wind and various head and tail wind shear conditions. Comparison of these responses can readily be made with the track characteristics of the presently used  $\dot{h}$  system by comparing Figure 3 to Figure 4. It was found that the proposed system offers considerably better track characteristics in heavy shears. Improved damping in the presence of tail winds is also evident.

The glide slope capture and track performance of the proposed system under FAA specified turbulence levels and various wind conditions is shown in Figure 5. The system has demonstrated good tracking capabilities under all of these conditions.



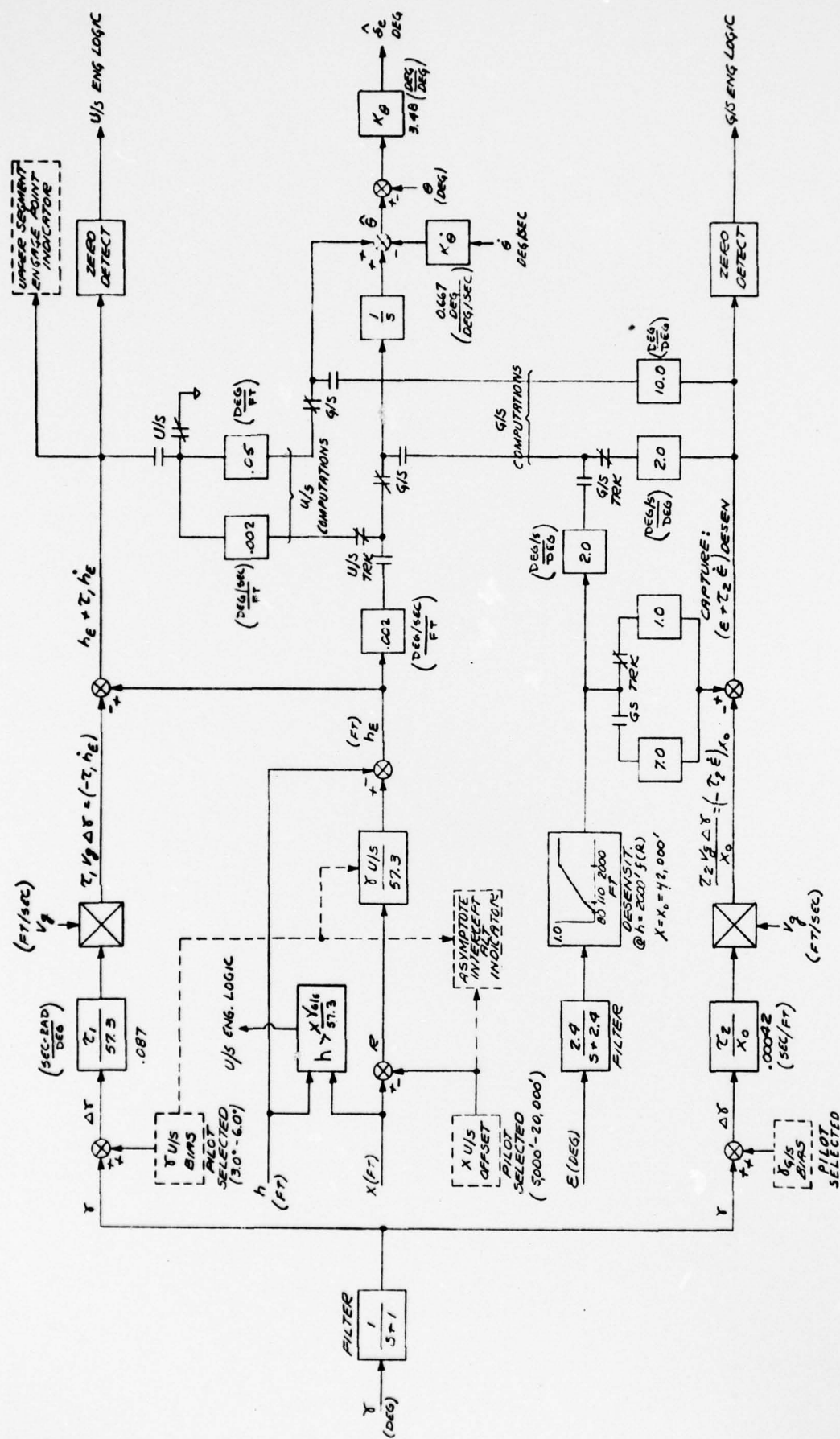


FIGURE 2. TWO SEGMENT APPROACH CONFIGURATION

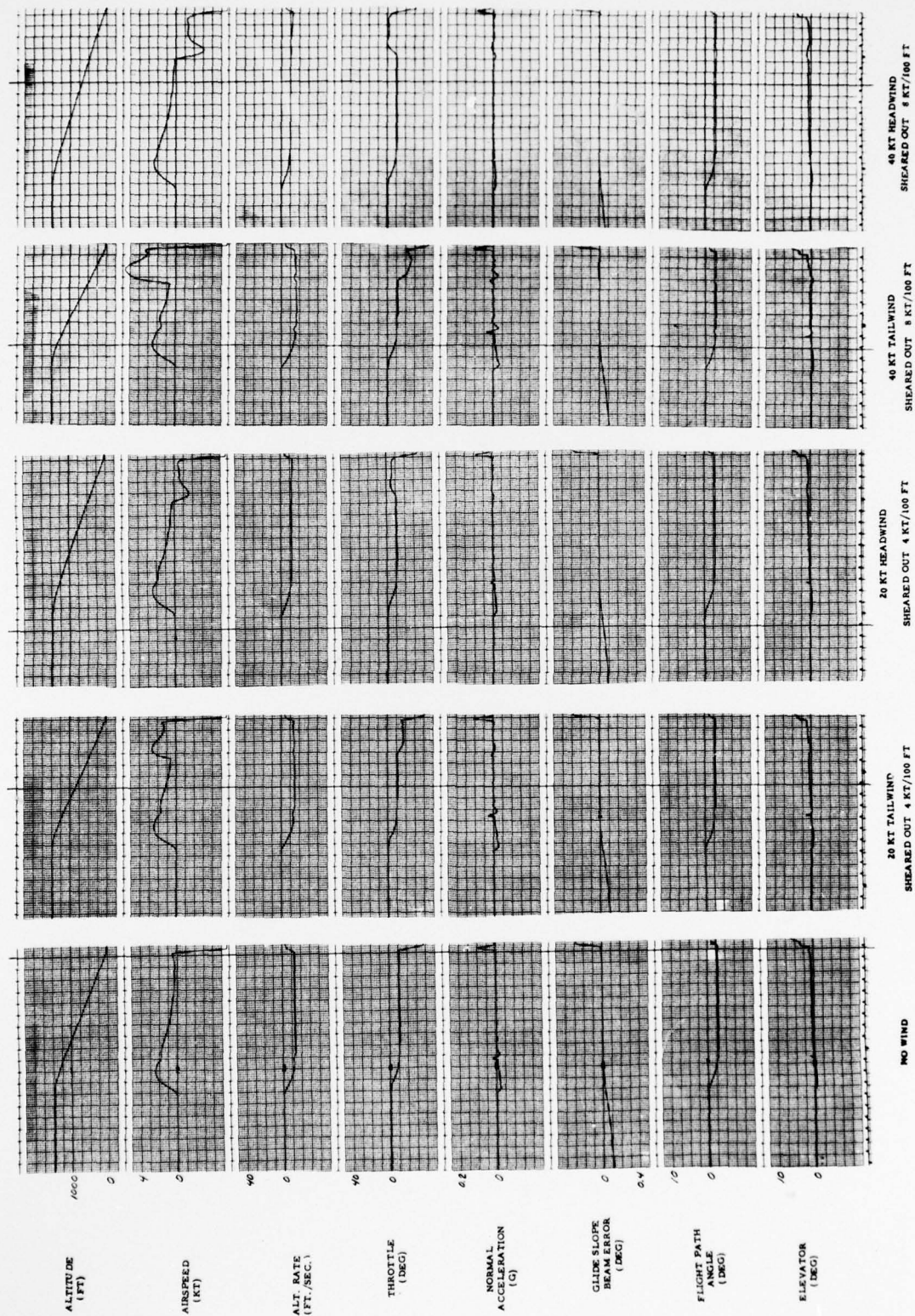


FIGURE 3. GLIDE SLOPE CAPTURE AND TRACK

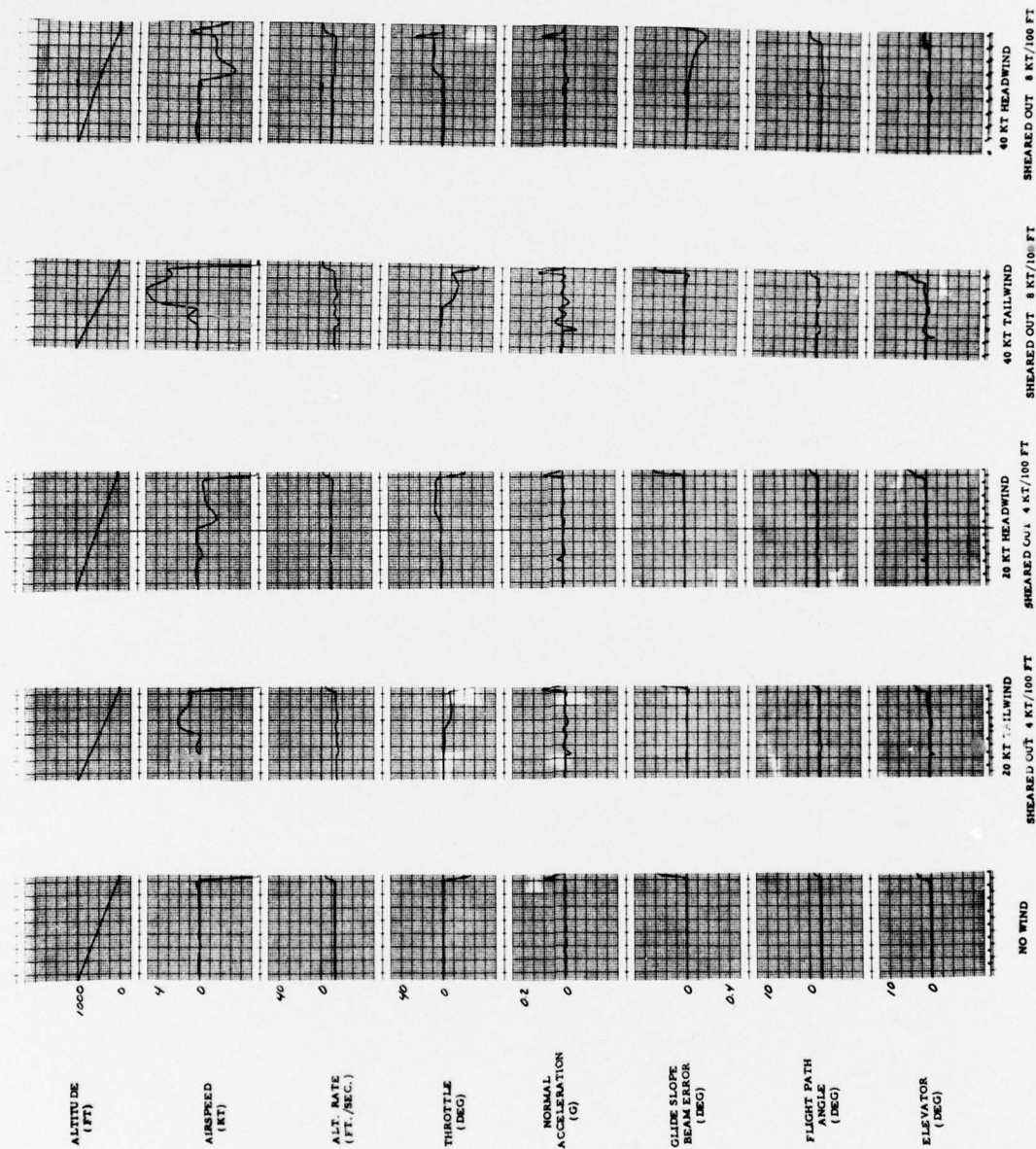


FIGURE 4. GLIDE SLOPE TRACK RESPONSE (PREVIOUS CONFIGURATION)



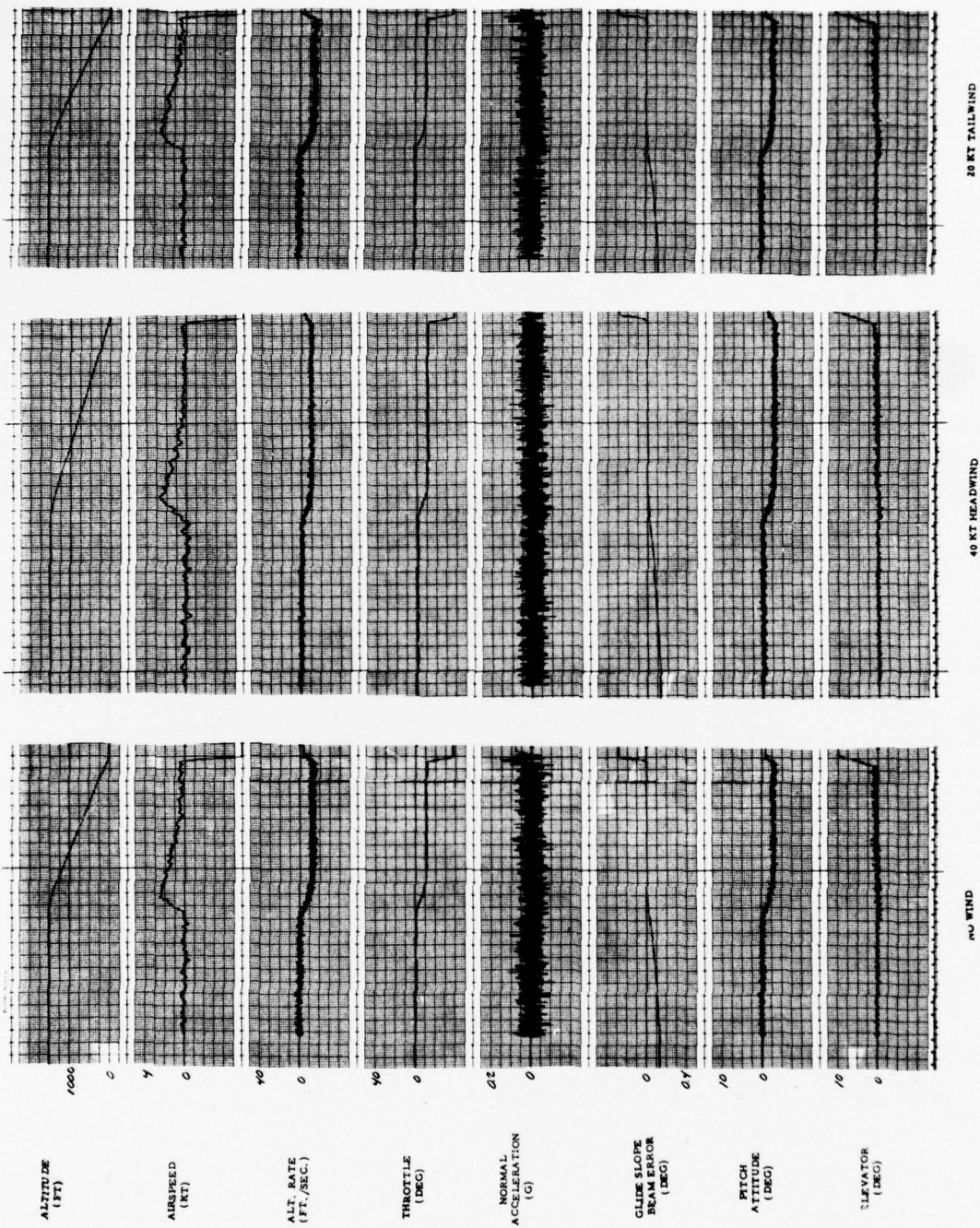


FIGURE 5. GLIDE SLOPE TURBULENCE RESPONSE

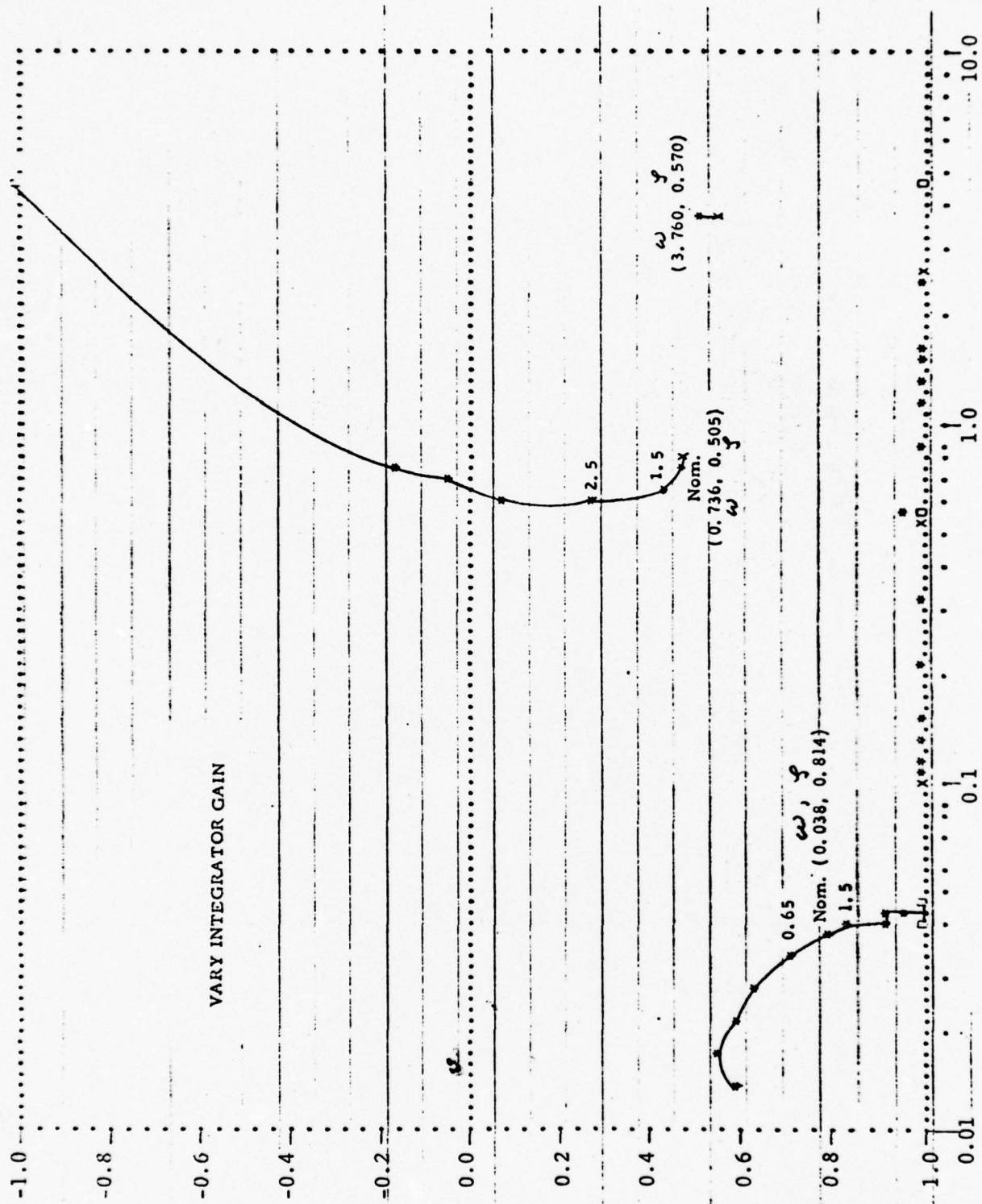


Figures 6 through 11 show the root loci of the glide slope capture and track modes at typical altitudes of 1200 feet and 400 feet respectively. Loci are plotted for variations in forward loop integrator gain, displacement gain and control law time constant. These loci demonstrate the stability of the capture and track modes and their sensitivity to variations of the above parameters. In some cases the loci suggest a possibility for further improvement in stability, although all nominal gain margins do appear adequate. It must be remembered, however, that the system's time response is also a criterion and often a compromise must be made in the choice of various parameter gains.

Figures 12 and 13 depict the upper segment captures from below and above, upper segment track to intercept glide slope at 1000 feet altitude and glide slope capture and track, under various wind conditions. In general the glide slope captures from above appear satisfactory. The upper segment capture and track from below also appear satisfactory, tracking the upper segment within 50 feet. The upper segment captures from above could possibly be improved by fine tuning. A 100 foot undershoot does occur, although this does not seem too extensive considering the altitudes at which it would occur.

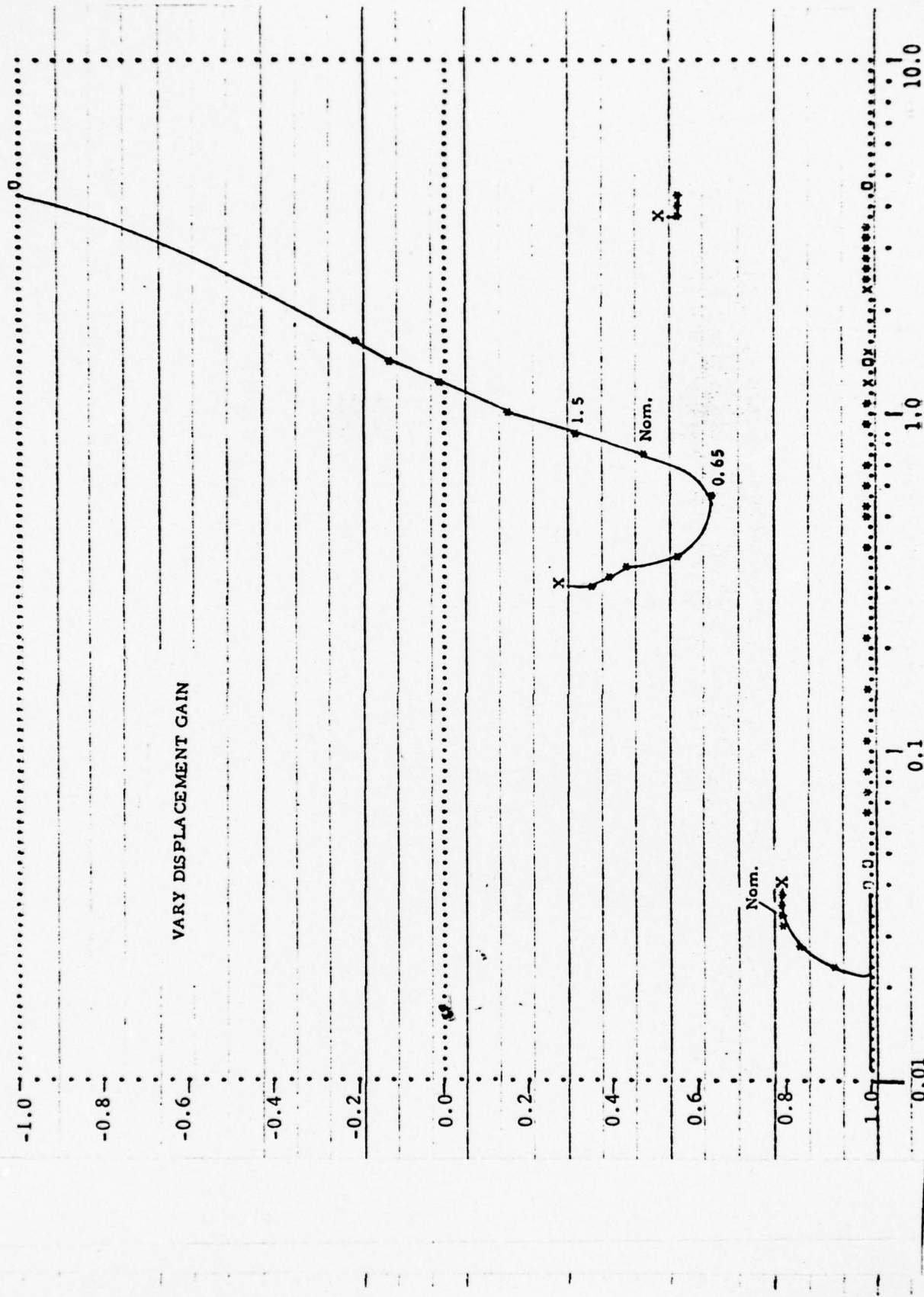
Figures 14 and 15 show upper segment captures close in and far out (segment intercepts of 500 and 1500 feet altitude) respectively, under various wind conditions. All cases demonstrated very little upper segment errors. The close in glide slope capture and track did display a slight increase in beam deviation. This area may also be subject to refinement in the near future.

Root loci demonstrating the stability and sensitivity to parameter variation of the upper segment capture and track modes are shown in Figures 16 through 21. As was the case in the glide slope root loci, the plots do demonstrate adequate gain margins for all parameters investigated.



ROOT LOCUS PLOT - ZETA VS. FREQUENCY (RAD/SEC)

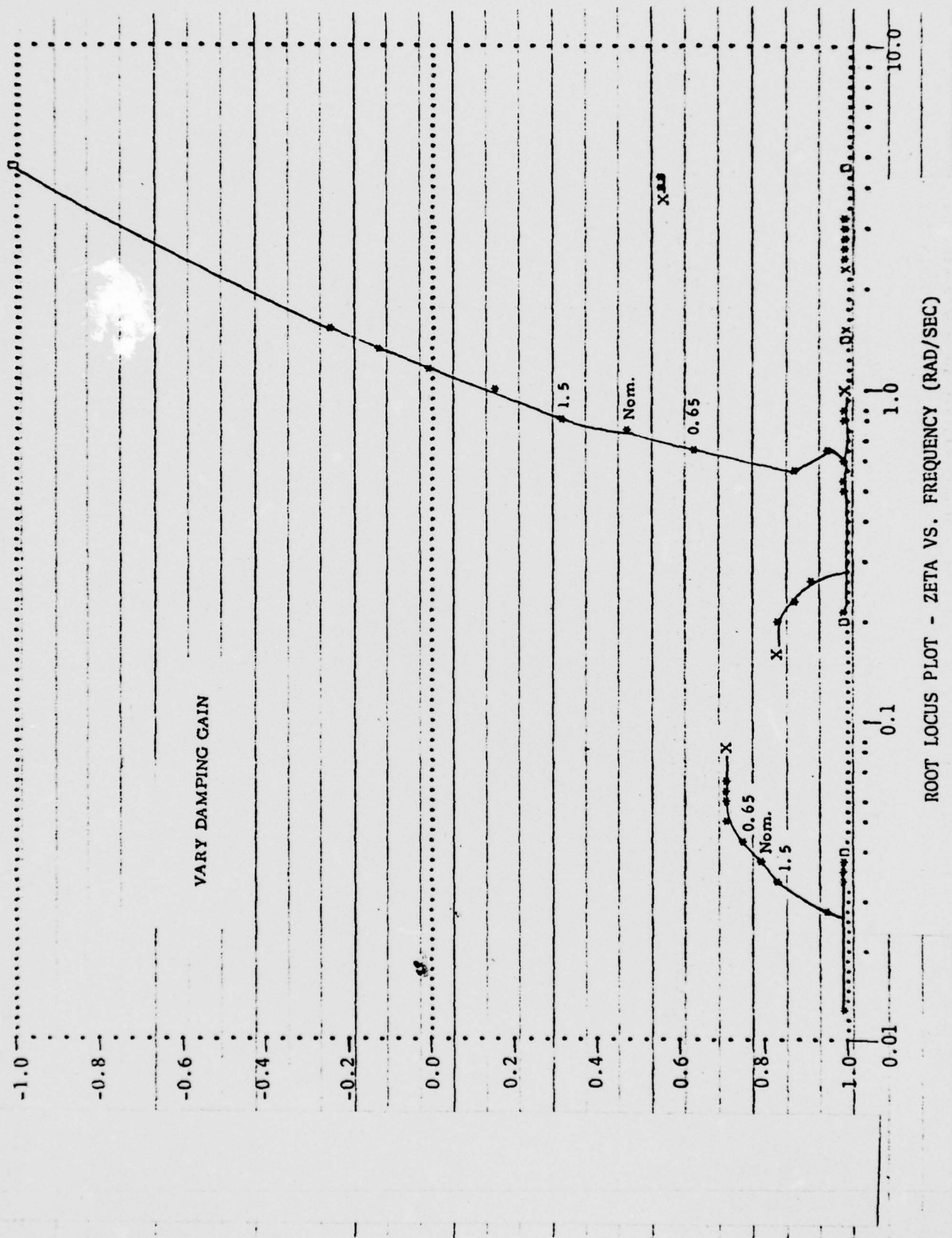
FIGURE 6. GLIDE SLOPE CAPTURE



ROOT LOCUS PLOT - ZETA VS. FREQUENCY (RAD/SEC)

FIGURE 7. GLIDE SLOPE CAPTURE

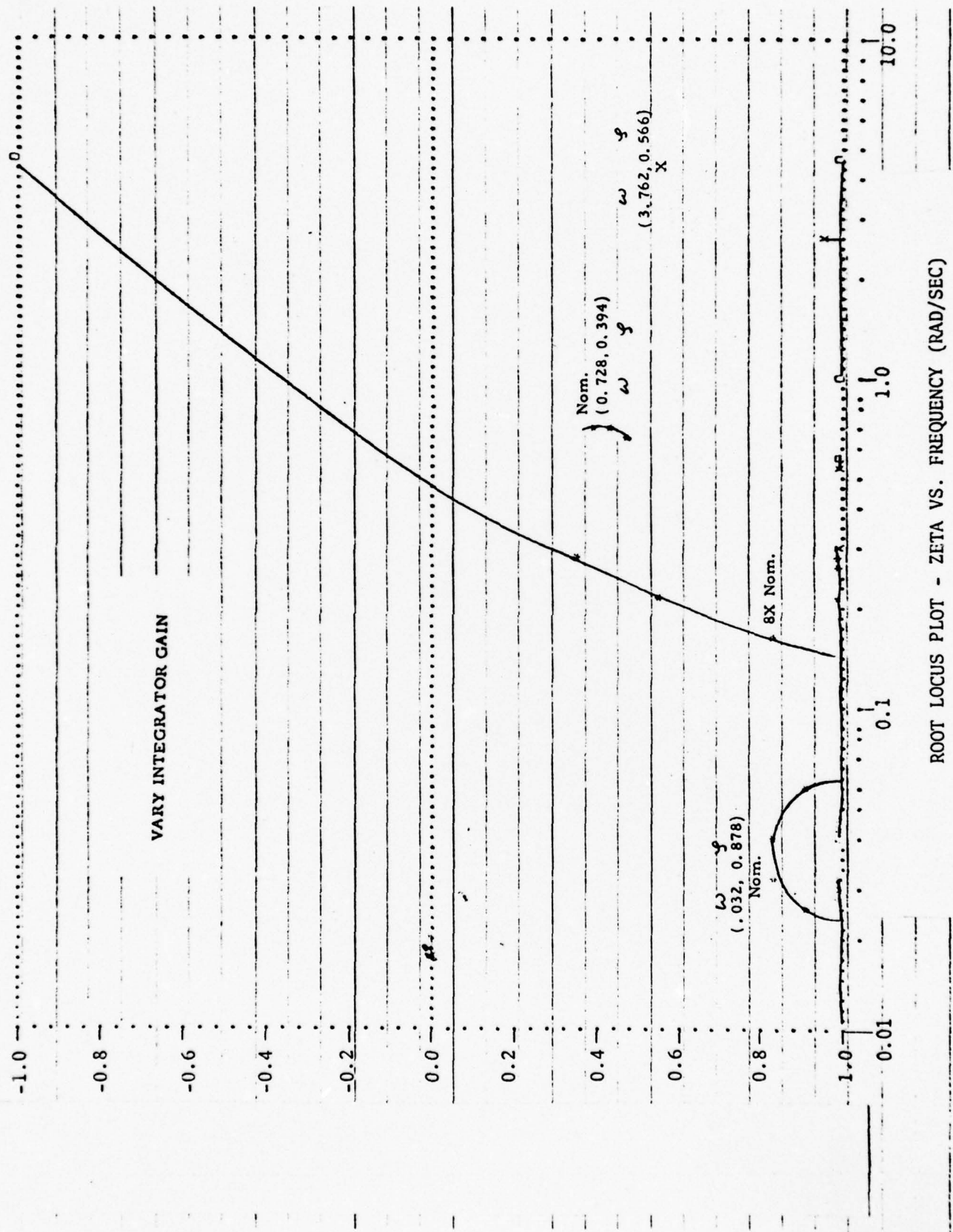




ROOT LOCUS PLOT - ZETA VS. FREQUENCY (RAD/SEC)

FIGURE 8. GLIDE SLOPE CAPTURE





ROOT LOCUS PLOT - ZETA VS. FREQUENCY (RAD/SEC)

FIGURE 9. GLIDE SLOPE TRACK

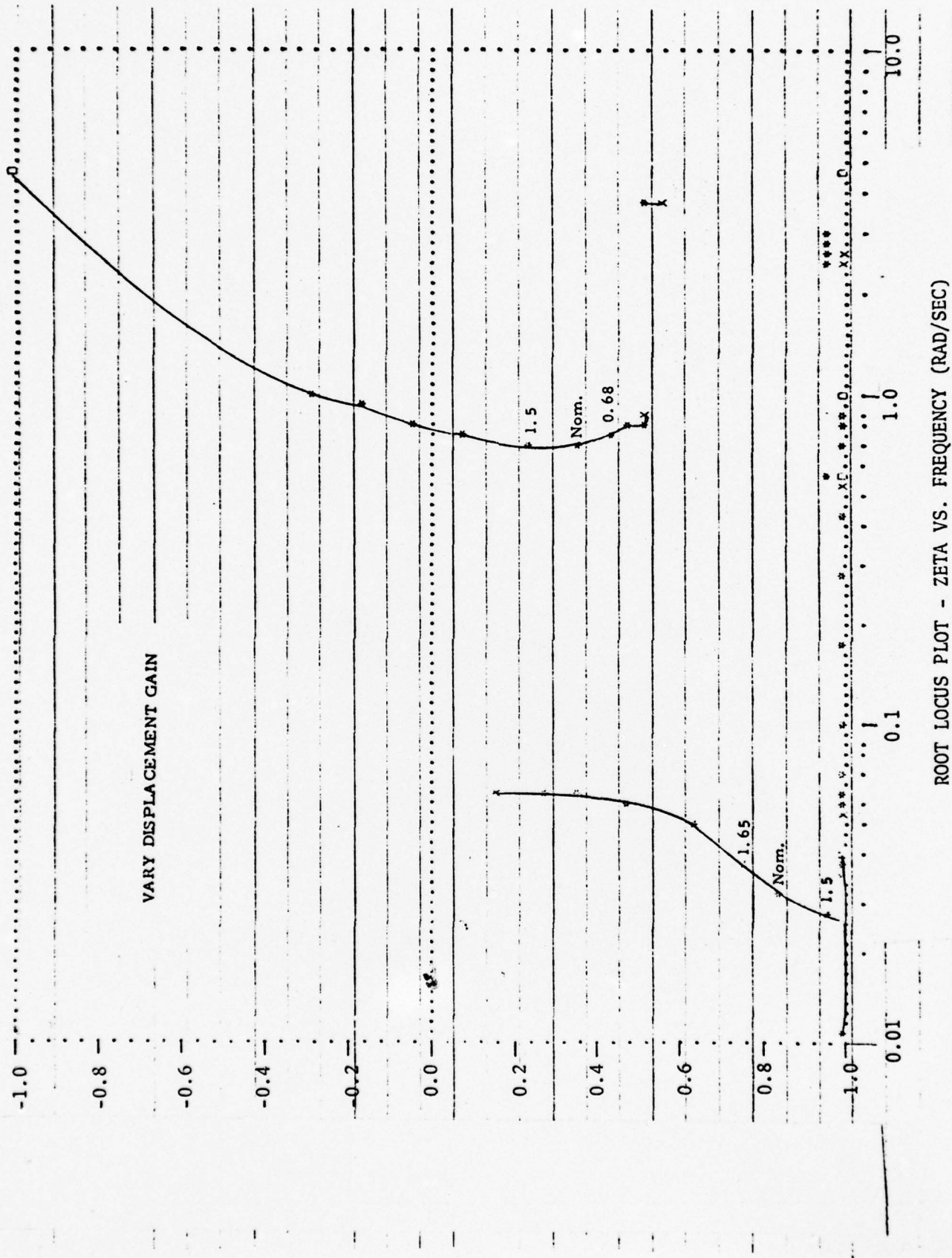
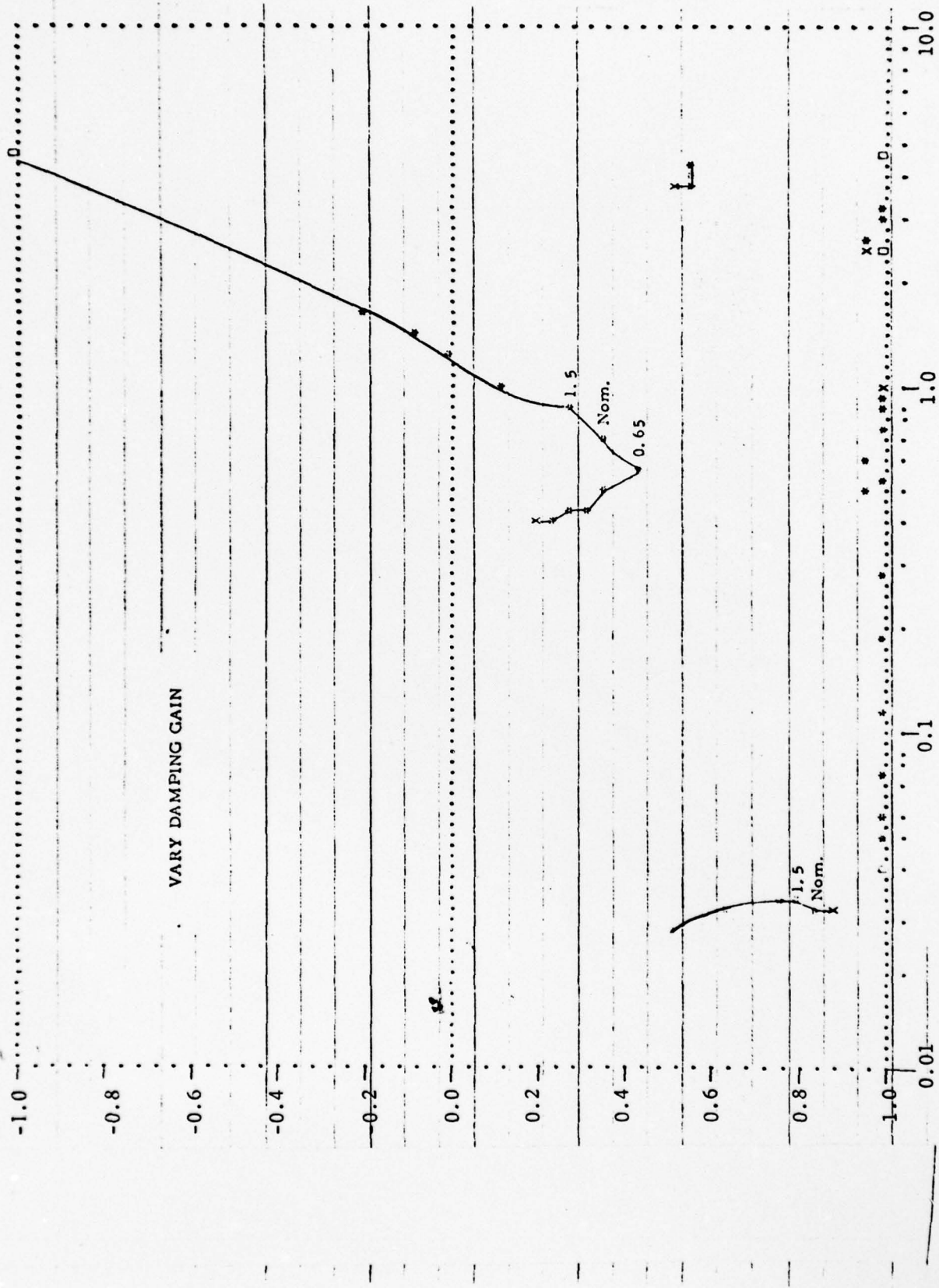


FIGURE 10. GLIDE SLOPE TRACK



ROOT LOCUS PLOT - ZETA VS. FREQUENCY (RAD/SEC)

FIGURE 11. GLIDE SLOPE TRACK



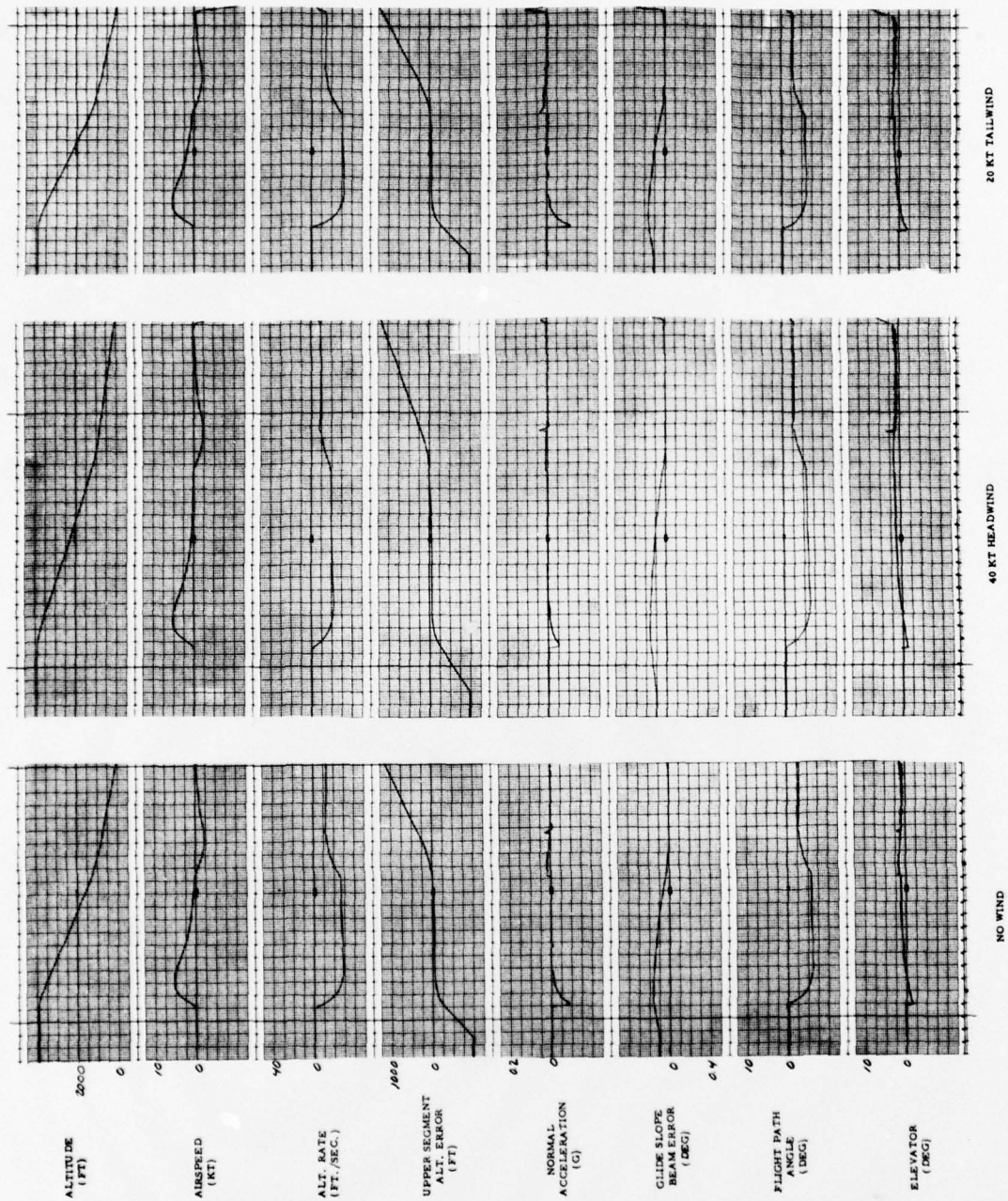


FIGURE 12. TWO SEGMENT CAPTURE AND TRACK (INITIAL INTERCEPT FROM BELOW)

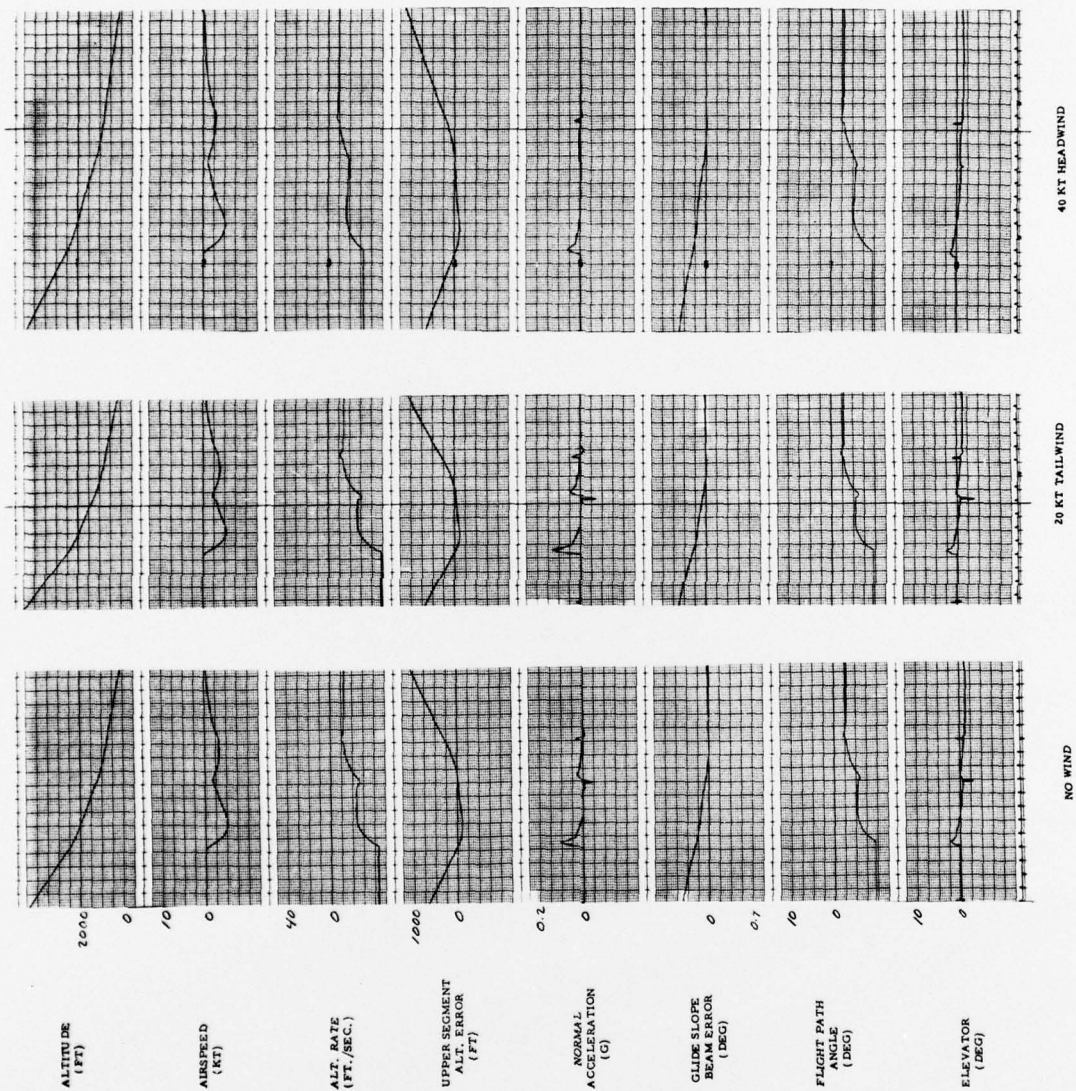


FIGURE 13. TWO SEGMENT CAPTURE AND TRACK (INITIAL INTERCEPT FROM ABOVE)

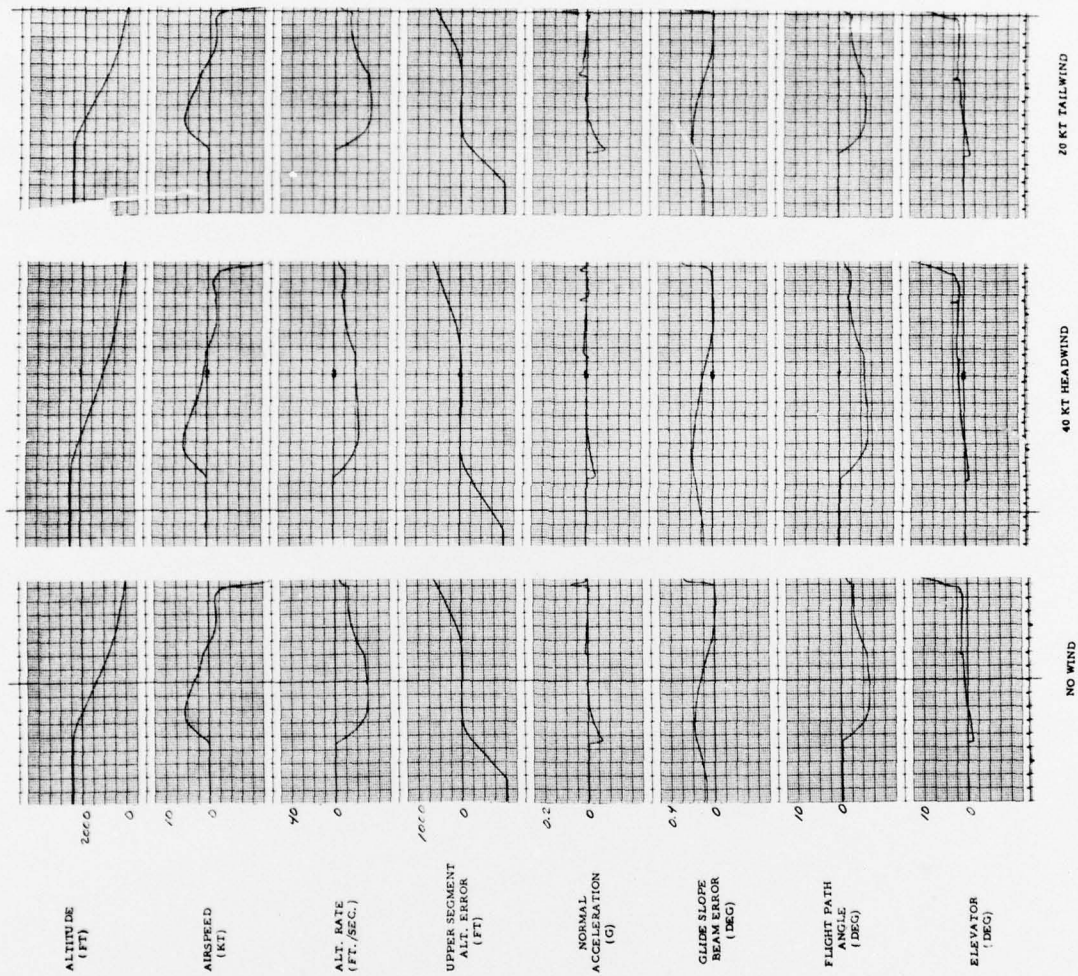


FIGURE 14. TWO SEGMENT CAPTURE AND TRACK (CLOSE IN)



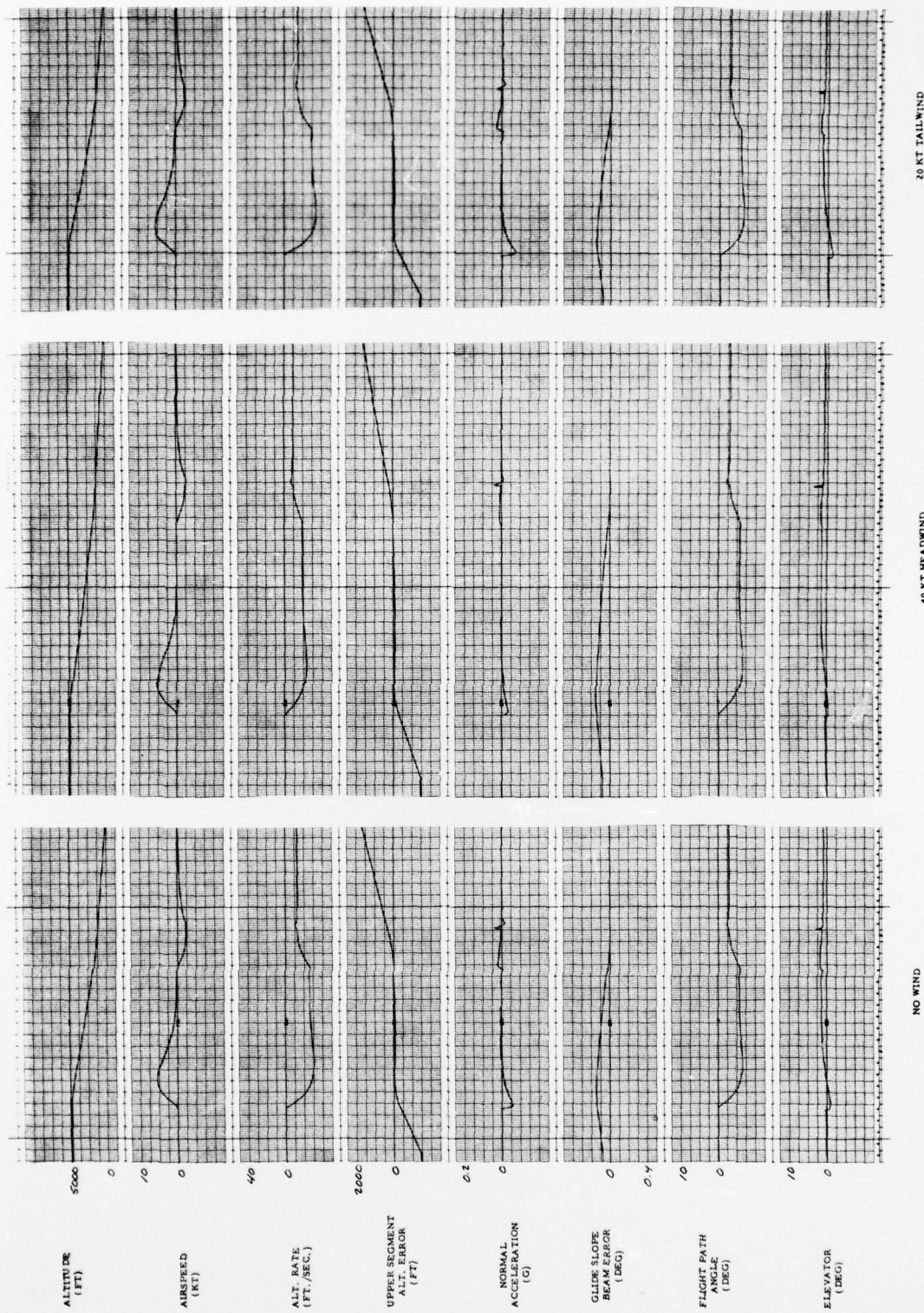
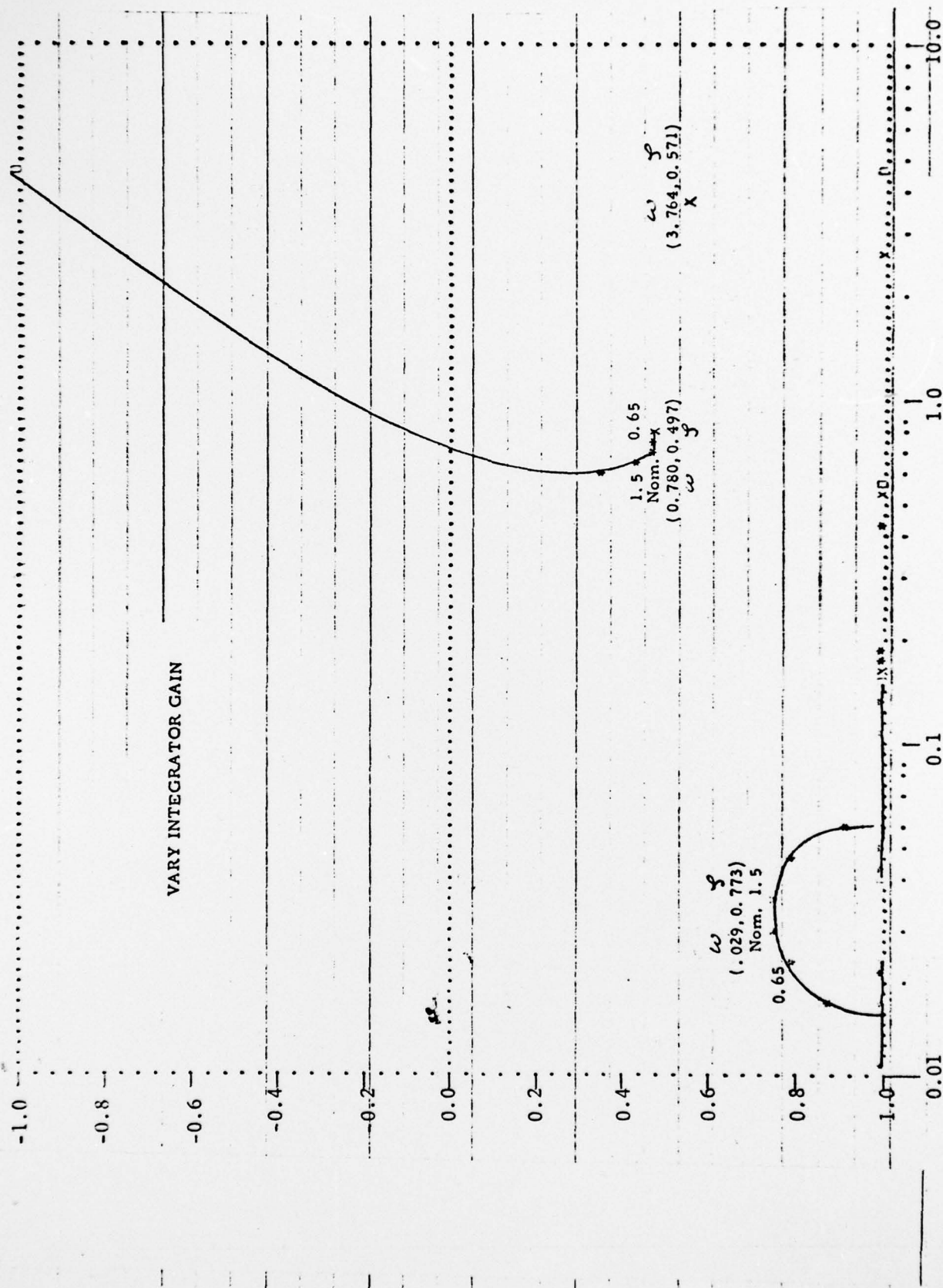
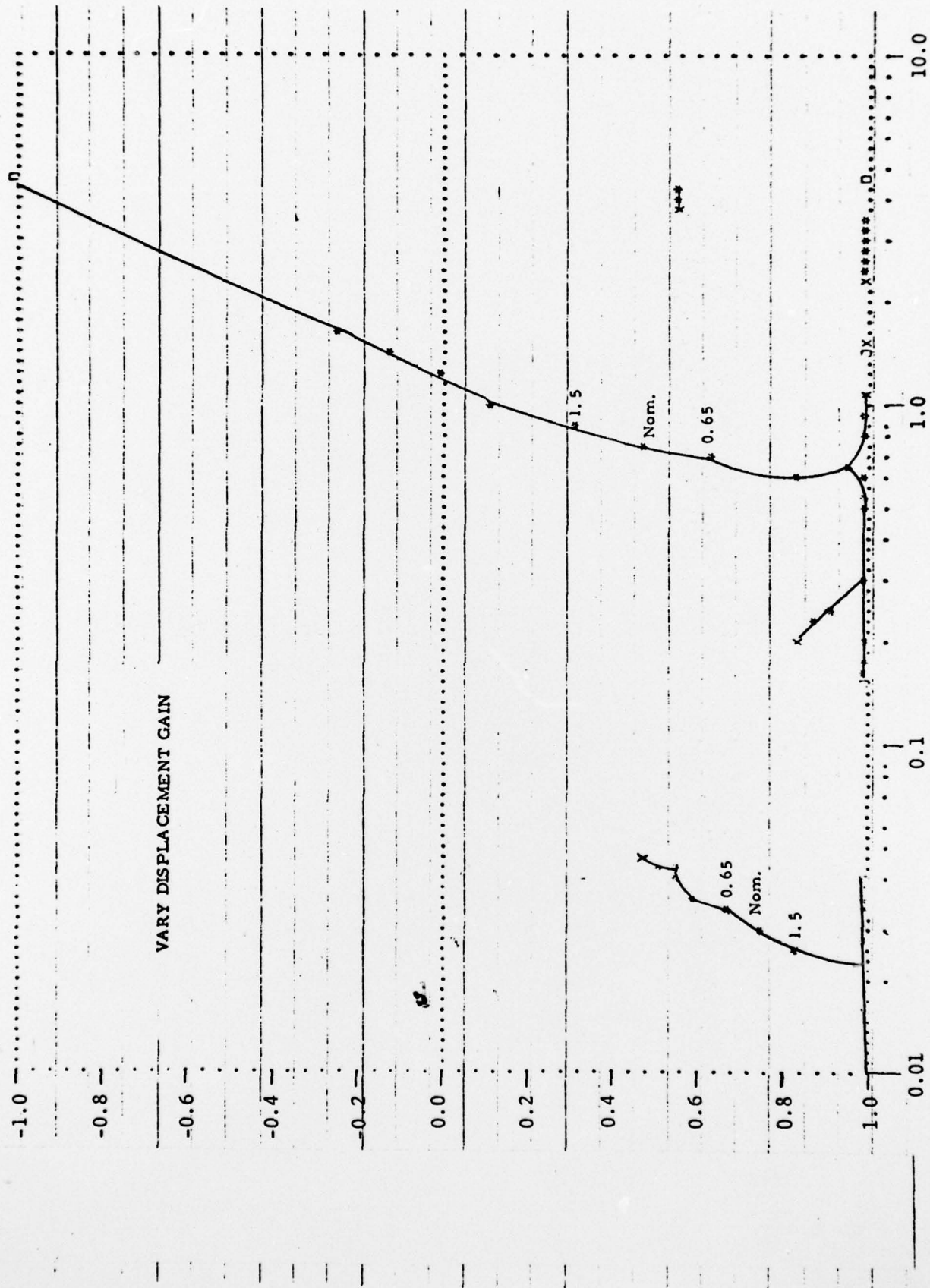


FIGURE 15. TWO SEGMENT CAPTURE AND TRACK (FAR OUT)



ROOT LOCUS PLOT - ZETA VS. FREQUENCY (RAD/SEC)

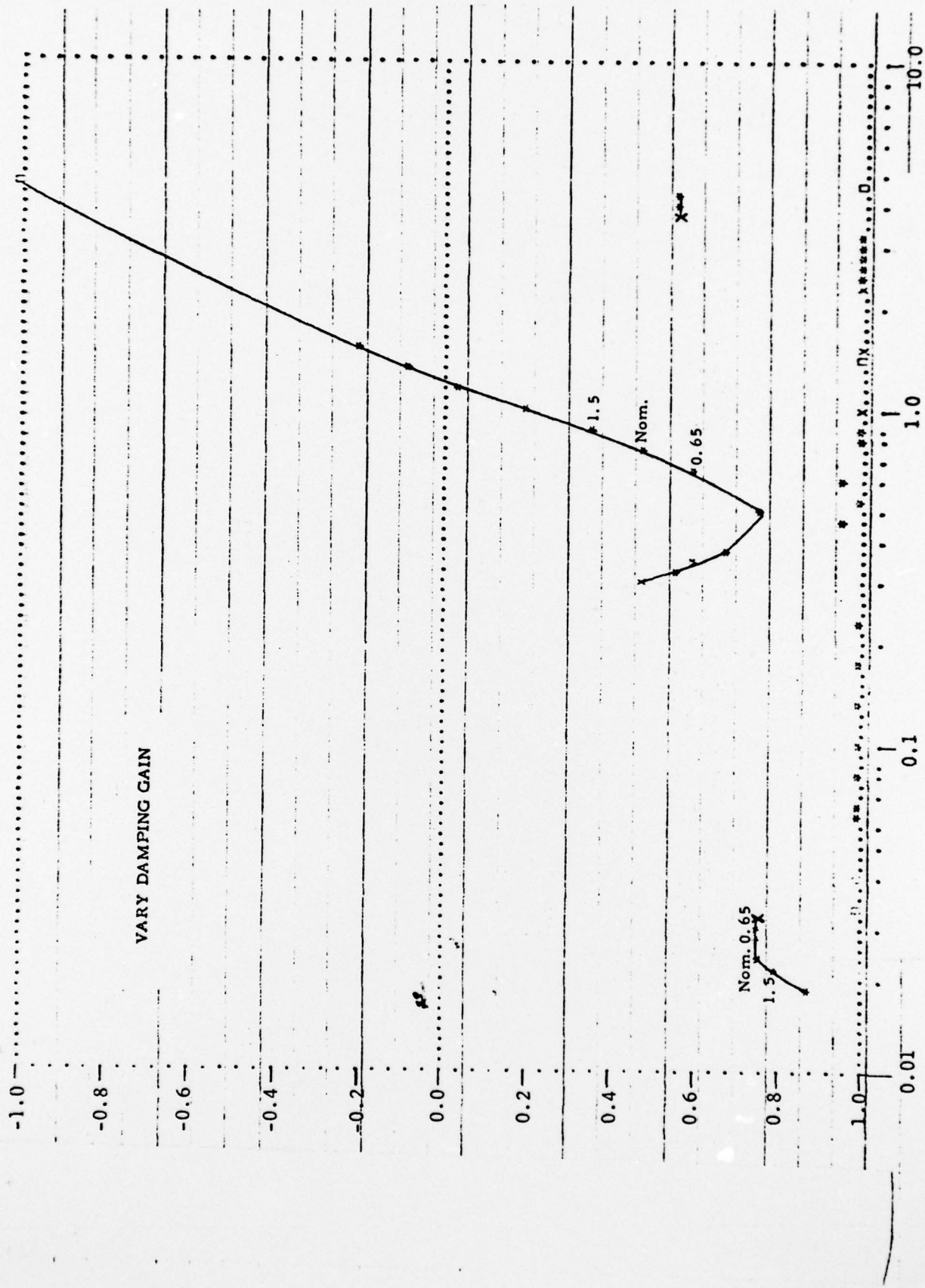
FIGURE 16. UPPER SEGMENT CAPTURE



ROOT LOCUS PLOT - ZETA VS. FREQUENCY (RAD/SEC)

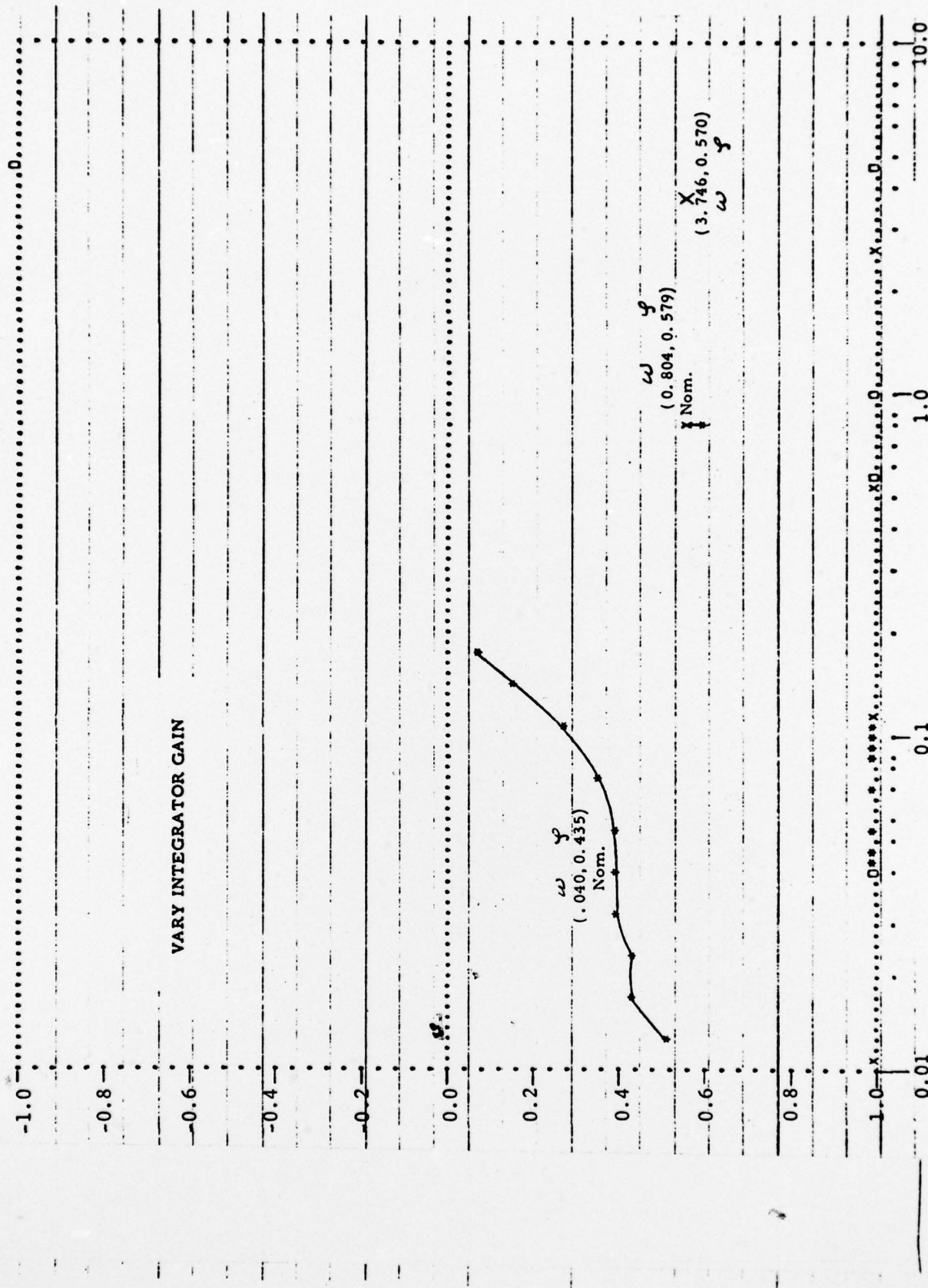
FIGURE 17. UPPER SEGMENT CAPTURE





ROOT LOCUS PLOT - ZETA VS. FREQUENCY (RAD/SEC)

FIGURE 18. UPPER SEGMENT CAPTURE



ROOT LOCUS PLOT - ZETA VS. FREQUENCY (RAD/SEC)

FIGURE 19. UPPER SEGMENT TRACK

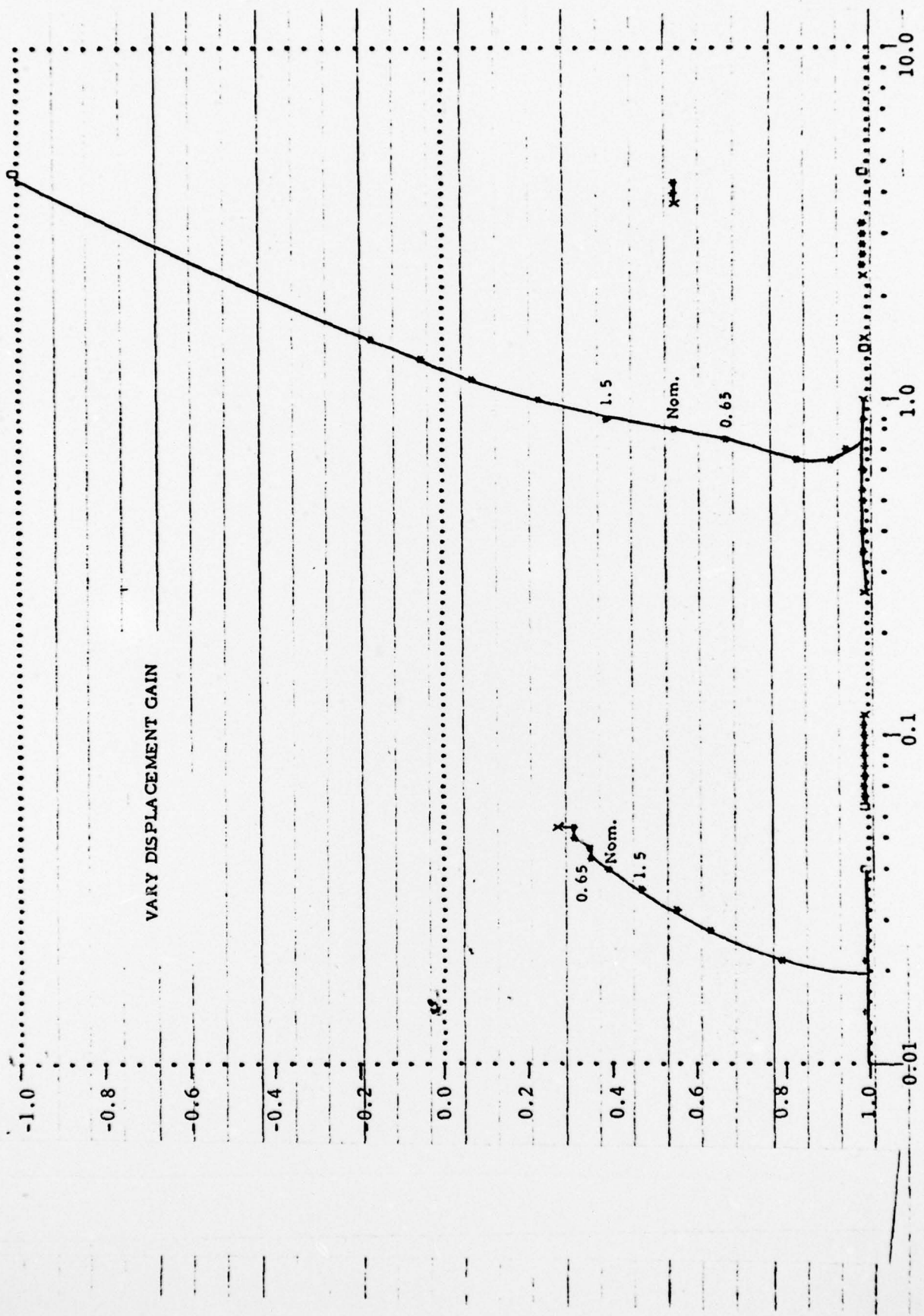
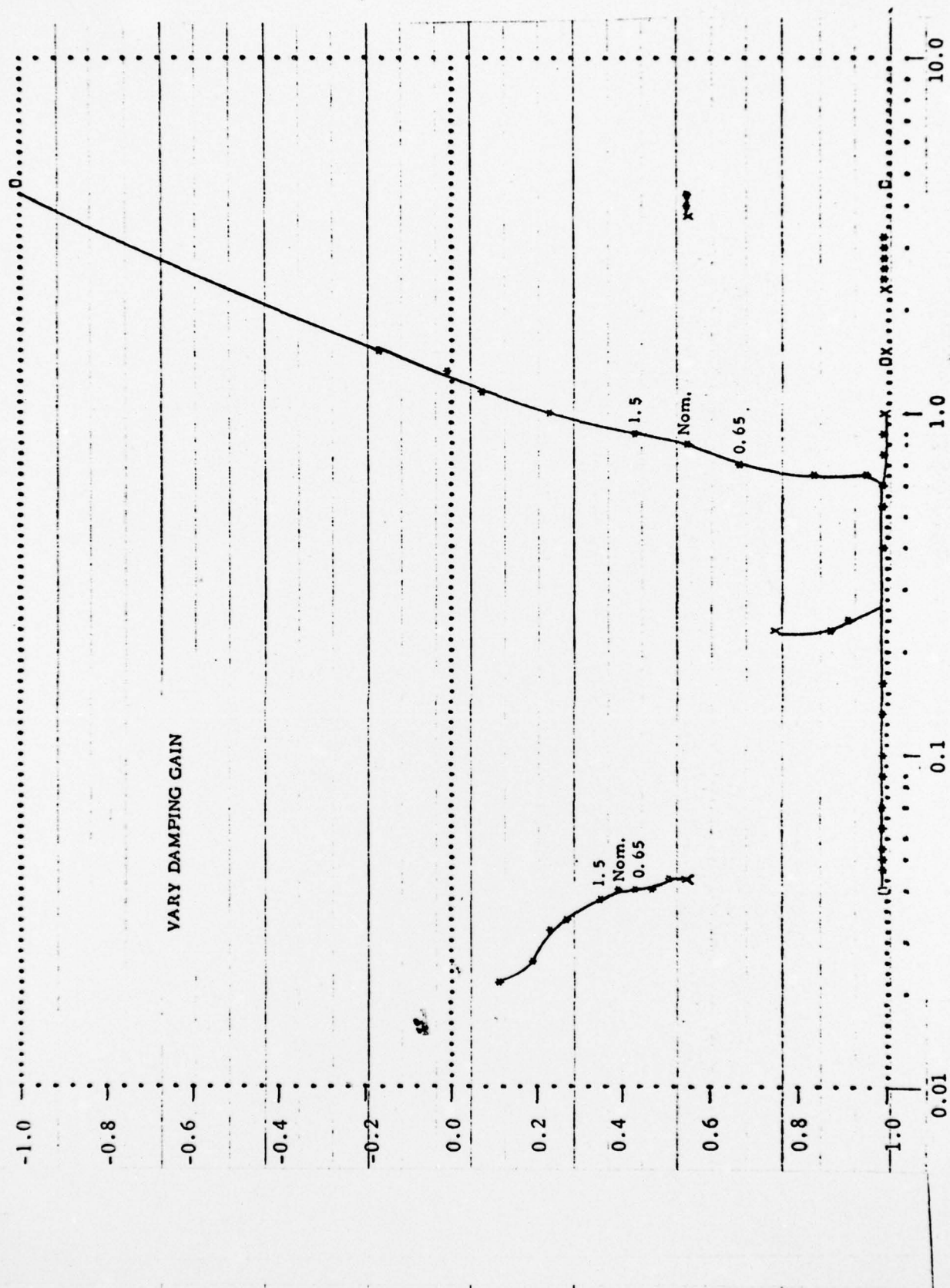


FIGURE 20. UPPER SEGMENT TRACK





ROOT LOCUS PLOT - ZETA VS. FREQUENCY (RAD/SEC)

FIGURE 21. UPPER SEGMENT TRACK

### SECTION 3

#### DEVELOPMENT OF SIMULATION

The following perturbation equations were used to simulate the three degree of freedom longitudinal axis.

$$\begin{aligned}\ddot{\theta} &= M_w \dot{w} + M_{\dot{w}} \dot{w} + M_q \dot{q} + M_u \dot{u} + M_{\delta T} \delta \dot{T} + M_{\delta e} \delta \dot{e} + M_H \dot{H} + M_{\delta s} \delta \dot{s} \\ \dot{w} &= z_w \dot{w} + z_{\dot{w}} \dot{w} + (V + z_q) \dot{q} + z_u \dot{u} + z_{\delta e} \delta \dot{e} + z_H \dot{H} \\ \dot{u} &= -g \theta + x_w \dot{w} + x_u \dot{u} + x_{\delta T} \delta \dot{T} + x_{\delta e} \delta \dot{e} + x_H \dot{H}\end{aligned}$$

Parameters are defined in Table 1.

The horizontal stabilizer, denoted above by  $\delta_s$ , was simulated with a time rate of 0.15 degrees of surface per second. It was engaged whenever elevator deflection exceeded 1.5 degrees. The effectiveness of the stabilizer in producing a pitching moment was taken to be three times that of the elevator.

The twelve flight conditions at which existing aero data was derived are not representative of the gross weight to airspeed ratio that is currently being flown on approach. For this reason, a new flight condition was developed with a gross weight of 160,000 pounds and airspeed of 155 knots. Table 1 shows the dimensional stability derivatives obtained from Wright Field for Flight Condition 2 defined with the same gross weight mentioned above, but an airspeed of 140 knots. The values for derivatives in the new flight condition were obtained by multiplying by the appropriate factor, 155/140 or  $(155/140)^2$  as shown in the table. For uniformity, this flight condition was simulated throughout the longitudinal study.

Winds simulated on the glide slope were constant until an altitude of 500 feet at which point they were steadily sheared to zero at zero altitude.

All quantities other than altitude and beam error are perturbation quantities whose values are zero at glide slope engage. The trim values of pitch attitude and angle-of-attack prior to glide slope will vary with conditions and must be added to the quantities shown here.

FIGURE 14. LONGITUDINAL DIMENSIONAL STABILITY DERIVATIVES

<u>Parameter</u>	<u>Definition</u>	<u>Value at Flight Condition 2</u>	<u>Value this Flight Condition</u>
$M_w$	$\frac{\rho s V \bar{c}}{2I_y} C_{m_\alpha}$	$-.6219 \times 10^{-2}$	$-.6916 \times 10^{-2}$
$M_{\dot{w}}$	$\frac{\rho s \bar{c}^2}{4I_y} C_{m_{\dot{\alpha}}}$	$-.1466 \times 10^{-2}$	$-.1466 \times 10^{-2}$
$M_q$	$\frac{\rho s V \bar{c}^2}{4I_y} C_{m_q}$	$-.8554$	$-.9512$
$M_u$	$\frac{\rho s V \bar{c}}{I_y} (C_{m_\alpha} + C_{m_u})$	$0$	$0$
$M_{\delta T}$	$\frac{z_j}{I_y}$	$.1852 \times 10^{-5}$	$.1852 \times 10^{-5}$
$M_{\delta e}$	$\frac{\rho s V^2 \bar{c}}{2I_y} C_{m_{\delta e}}$	$1.124$	$1.390$
$M_H$	$\frac{\rho s V^2 \bar{c}}{2I_y} \Delta C_m$		$-.2576$
$Z_w$	$\frac{-\rho s V}{2m} (C_{L_\alpha} + C_D)$	$-.637$	$-.708$
$Z_{\dot{w}}$	$\frac{-\rho s \bar{c}}{4m} C_{L_{\dot{\alpha}}}$	$-.0105$	$-.0105$
$Z_q$	$\frac{-\rho s V \bar{c}}{4m} C_{L_q}$	$-6.15$	$-6.84$



<u>Parameter</u>	<u>Definition</u>	<u>Value at Flight Condition 2</u>	<u>Value this Flight Condition</u>
$Z_u$	$\frac{-\rho s V}{m} (C_L + C_{L_u})$	-.272	-.302
$Z_{\delta e}$	$\frac{-\rho s V^2}{2m} C_{L_{\delta e}}$	7.46	9.23
$Z_H$	$\frac{-\rho s V^2}{2m} \Delta C_L$		-5.113
$X_w$	$\frac{\rho s V}{2m} (C_L - C_{D\alpha})$	.0647	.0719
$X_u$	$\frac{-\rho s V}{m} (C_D + C_{D_u})$	-.0426	-.0474
$X_{\delta T}$	$\frac{1}{m}$	$.2013 \times 10^{-3}$	$.2013 \times 10^{-3}$
$X_{\delta e}$	$\frac{-\rho s V^2}{2m} C_{D_{\delta e}}$	1.49	1.84
$X_H$	$\frac{-\rho s V^2}{2m} \Delta C_D$		1.812
$M_{\delta s}$	$3 M_{\delta e}$	3.372	4.170

## SECTION 4

### CONCLUSION

This study has investigated a design approach using inertial flight path information as a damping term during glide slope capture and track. A comparison was made between it and the present system using sink rate as the damping term during track.

The flight path angle damped system with its exponential capture can be used under a wide range of intercept and wind conditions without the customary beam overshoot. In addition a significant improvement in the aircraft's ability to track the glide slope beam in heavy wind shears and turbulence is evident.

The feasibility of extending the above capture and damping technique to control an aircraft along a pilot selected upper segment, to intercept the glide slope, was also demonstrated. The conformance to a preselected path in space was computed through the use of range and altitude information in the absence of a fixed beam.